Removal of ferrous and manganous from water by activated carbon obtained from sugarcane bagasse

Khalid Z. Elwakeel[a,*], Gamal O. El-Sayed[b], Susan M. Abo El-Nassr[c]

[a]Faculty of Science, Environmental Science Department, Port-Said University, Port-Said, Egypt, Tel. +20 1061694332;
email: khalid_elwakeel@sci.psu.edu.eg
[b]Faculty of Science, Chemistry Department, Benha University, Benha, Egypt, email: gamaloelsayed@yahoo.com
[c]Water Quality Audit Department, Holding Company for Water and Wastewater, Cairo, Egypt, email: ahmad_t174@yahoo.com

ABSTRACT

Activated carbon was prepared from sugarcane bagasse impregnated with phosphoric acid at 500°C activation temperature and 2 h activation time, resulting in the carbon yield of 27.13%. The prepared activated carbon has high BET surface area (671.54 m^2/g) and the maximum adsorption of iodine is 602.23 mg/g. The adsorption characteristics of the obtained carbon towards both Fe(II) and Mn(II) at different experimental conditions were conducted by means of batch and column methods. The adsorbent showed high affinity for the removal of both Fe(II) or Mn(II) from aqueous medium, where an uptake values of 7.01 and 5.40 mg/g were reported for Fe(II) and Mn(II), respectively, at 25°C. Various parameters such as pH, agitation time and speed, adsorbent dose, metal ion concentration, temperature, and ionic strength had been studied. The kinetic and thermodynamic behavior of the adsorption reaction was defined, these data indicated pseudo-second-order model and the adsorption is endothermic in nature and mainly physical. Breakthrough curves for the removal of Fe(II) or Mn(II) were studied. Regeneration and durability of the loaded carbon toward the successive cycles were clarified. The adsorbed Fe(II) or Mn(II) was eluted from the column effectively using 0.5 M hydrochloric acid.

Keywords: Iron and manganous; Removal; Adsorption; Kinetics; Column method

1. Introduction

Groundwater is the major source of domestic water for people living in rural and semi-urban areas in Egypt. Iron and manganese are common metallic elements found in the earth's crust [1]. Water percolating through soil and rock can dissolve minerals containing iron and manganese and hold them in solution. Iron and manganese removal is the most common type of municipal water treatment in Delta of Egypt. Neither of the elements causes adverse health effects; they are, in fact, essential to the human diet [2]. However, water containing excessive amounts of iron and manganese make the water unusable mainly for esthetic considerations such as discoloration, metallic taste, odor, turbidity, staining of laundry, and plumbing fixtures [3]. The presence of these elements in water can influence the development of ferruginous and manganese bacteria on walls of pipes. The growing micro-organisms cause corrosion of pipes [4].

*Corresponding author.

Therefore, the World Health Organization has set a guideline value of 0.3 and 0.4 mg/L of iron and manganese in drinking water [5], and many countries have adopted this value in their national drinking water quality standards including Egypt. Traditional methods used for the removal of Fe(II) and Mn(II) from groundwater in public water supply systems in different Egyptian governorates are aeration and filtration, as well as oxidation with oxidizing agents such as chlorine and potassium permanganate [6], other methods available for Fe(II) and Mn(II) removal include oxidation/precipitation, coagulation/coprecipitation, nanofiltration, reverse osmosis, electrodialysis, adsorption, ion exchange, foam flotation, solvent extraction, and bioremediation [7,8].

The search for an adsorbent with characteristics such as high adsorption capacity, long life, readily available in bulk quantities, and cost-effective is an important issue. Extensive research has been carried out during the last 10 years to find such adsorbents for the removal of metal ions [9–12]. A number of low-cost agricultural wastes, such as mud and fly ash, have been used for the removal of a range of metal ions [13,14]. Several natural resources have also been studied including tree fern, peat coal, and chitosan [15–17].

Activated carbon has received much attention in the recent years due to its versatile application in adsorption science. Generally, activated carbon is prepared by physical and chemical activation methods. Activated carbon, a tasteless, solid, microcrystalline, and non-graphitic form of black carbonaceous material with a porous structure, has been regarded as a unique and versatile adsorbent because of its extended surface area, microporous structure, high adsorption capacity, and high degree of surface reactivity [18,19]. Activated carbon is excellent adsorbent for purifying, filtering, bleaching, deodorizing, de-chlorination, de-intoxication, removal or modification of taste, and the concentration of liquid and gas materials [20].

Adinaveen et al. studied the preparation of activated carbon composite from sugarcane bagasse [21]. The prepared activated carbon showed good electro-chemical property and when treated with H_3PO_4, it has the effect of producing considerable quantities of micropores. It is important to develop technologies available for water treatment. Generally, these technologies should be cost-effective, highly efficient, and easy to handle. Foo et al. evaluated the sugarcane bagasse-derived activated carbon prepared by microwave heating for the adsorptive removal of ammonical nitrogen and orthophosphate from the semi-aerobic landfill leachate [22]. The results revealed the feasibility of the sugarcane bagasse developed adsorbent for the adsorptive treatment of semi-aerobic landfill leachate.

In the present study, we report the production of activated carbon from sugarcane bagasse using H_3PO_4 and its application for the removal of Fe(II) and Mn (II) from aqueous solutions. Batch and column methods were conducted to investigate the adsorption capacity of ferrous and manganese onto the obtained activated carbon. The influences of the experimental parameters such as pH, temperature, agitation time, adsorbent dose, and initial concentration on adsorption will be studied. The kinetic models used to describe the rate data will be discussed. Also desorption studies will be carried out using hydrochloric acid to regenerate the spend adsorbent.

2. Experimental

2.1. Preparation of activated carbon

The precursor material of sugarcane bagasse was first cracked and crushed to free the pitch and light chaff in a hammer mill, then the sample was heated at 400°C for about 4 h and cooled down to room temperature. The resulting carbon (pre-activation carbon) was then subjected to chemical activation (for the purpose of creating porous structure in the carbon matrix) with 45% H_3PO_4 solution for 24 h with an impregnation ratio of 2.0. The impregnation ratio was defined as:

$$\text{The impregnation ratio} = \frac{\text{Weight of phosphoric acid in solution}}{\text{Weight of bagasse}}$$

(1)

The resulting impregnated carbon was then subjected to heat treatment in a furnace (Thermo Scientific Lindberg/Blue M LGO Box) at 500°C for 2 h. After heat treatment the activated carbon was washed with 10% hydrochloric acid to remove the ash, then it was washed several times with hot water to remove the excess acids. The washed sample was dried at 110°C to get the final product (activated carbon).

2.2. Production yield

The yield of the activated carbon is defined as the ratio of the Weight of the resulting activated carbon to that of the original sugarcane bagasse, with both weights being measured on a dry basis.

2.3. The texture properties

The texture characteristics of the activated carbon were determined by N_2 adsorption at 77 K, using an

Autosorb I (Quantachrome Micrometrics, USA), computer-controlled apparatus. The total surface area was estimated by applying BET equation, and total pore volume determined from nitrogen held as liquid as $P/P_o = 0.95$, and the average pore diameter were evaluated [23].

2.4. The iodine number

The iodine number was calculated, employing a four-point Freundlich isotherm. The iodine residual concentration was determined by titration with standard $Na_2S_2O_2$ solution.

2.5. Determination of point of zero charge

Batch equilibrium method for determination of the point of zero charge (PZC) was proposed by Noh and Schwarz [24]. Accordingly, the samples of activated carbon (0.2 g) were shaken in PVC vials, for 24 h, with 40 mL of 0.1 mol/L KNO_3, at different initial pH values. Initial pH values were obtained by adding an amount of KOH or HNO_3 solution (0.1 mol/L), keeping the ionic strength constant. The amount of H^+ or OH^- ions adsorbed by activated carbon was calculated from the difference between the initial and the final pH.

2.6. Preparation of solutions

A stock solution (10 mg/L) of ferrous chloride or manganous chloride was prepared in distilled water. The desired concentrations were then obtained by dilution. HCl (0.5 M) and NaOH (0.5 M) were used to change the acidity of the medium. About 0.5 M of HCl acid was used for elution of Fe(II) or Mn(II) from the adsorbent. The concentration of Fe(II) and Mn(II) was measured using spectrophotometric method. 1,10-phenanthroline method was used for ferrous determination at 510 nm, while the concentration of manganous ion was estimated at 525 nm using periodate oxidation method [25]. The measurements were taken on a CECIL CE 7400 Double Beam UV/VIS spectrophotometer, England.

2.7. Batch experiments for adsorption of Fe(II) and Mn(II)

Adsorption of Fe(II) or Mn(II) under controlled pH was carried out by placing 0.05 g of dry carbon in a series of flasks each contains 50 mL of 10 mg/L of Fe(II) or Mn(II) solution. The flasks were conditioned on a shaker at 4 rpm 25°C. The uptake of Fe(II) or Mn(II) was calculated by determining the residual concentration of Fe(II) or Mn(II) following the above method.

The effect of initial concentration of Fe(II) or Mn(II) on the adsorption was studied by placing 0.05 g portions of dry carbon in a series of flasks each contains 50 mL of Fe(II) or Mn(II) with different concentrations at normal pH. The contents of the flasks were equilibrated on the shaker (Model: VRN-360) at 4 rpm and at 25, 35, and 45°C for 30 min. After equilibration, final concentrations and pH of Fe(II) or Mn(II) for all flasks were measured.

2.8. Column method

2.8.1. Column loading

Flow experiments were performed in a plastic column (length 10 cm and diameter 0.5 cm). A small piece of glass wool was placed at the bottom of the column and then a known quantity of the activated carbon was placed in the column. A known quantity of the adsorbent under investigation was placed in the column to yield the desired bed height. Fe(II) or Mn(II) solution having an initial concentration of 10 mg/g was flowed downward through the column at flow rate of 2 mL/min. Samples were collected from the outlet of the column at different time intervals and analyzed for Fe(II) or Mn(II) ion concentration. The operation of the column was stopped when the outlet metal ion concentration matches its initial concentration.

2.8.2. Regeneration of the column

The adsorbent bead loaded by Fe(II) or Mn(II) was then subjected for regeneration using 50 mL 0.5 M of hydrochloric acid. The adsorbent was then carefully washed with distilled water to become ready for the second run of loading with Fe(II) or Mn(II). The regeneration efficiency (RE%) was calculated according to the following equation:

$$RE\% = \frac{\text{Uptake in the second run}}{\text{Uptake in the first run}} \times 100 \qquad (2)$$

3. Results and discussion

3.1. Physical properties of the activated carbon

Fig. 1 represents nitrogen adsorption isotherm at 77 K of the activated carbon prepared from sugarcane bagasse. The isotherm exhibited a typical type I isotherm according to IUPAC classification, with a well-defined plateau pointing to microporous structures.
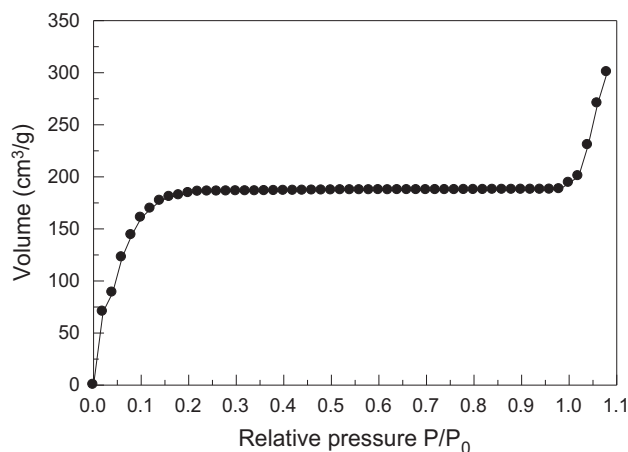
Fig. 1. Nitrogen adsorption isotherm of the activated carbon.

The initial (steepest) part of the isotherm represents the micropore filling (rather than the surface coverage) and a low slope of the plateau is an indicative of multilayer adsorption on the external surface. The rapid vertical rise near $P/P = 1$, can be identified as "cold spots" in the apparatus (which lead to bulk condensation of the gas and a false measure of adsorption in the volumetric method). Thus, the prepared activated carbon is considered to be microporous with a relatively small external surface area. The surface area parameters such as BET surface area, total pore volume, and average pore diameter were calculated and reported in Table 1. The BET surface area has high value of 671.54 m²/g. This value shall be attributed to the pores generated on the carbon and silica matrices. The phosphoric acid activation induces the chemical and structural alterations of the different constituent biopolymers of the precursors sugarcane bagasse, namely cellulose, hemicellulose, and lignin, leading to the development of extensive porous structures. The surface area of the prepared activated carbon was also confirmed from the iodine number (602.23 mg/g). The high value of the total pore volume obtained from N_2 (0.426 cm³/g) adsorption indicates that the use of H_3PO_4 has the effect of producing considerable quantities of micropores.

After the activation and washing, the carbon yield was 27.13%, as presented in Table 1. It was observed that there is a difference between the carbon yields between the pre-activation (35.34%) and after activation stage (27.13%). This was mainly due to the further removal of volatile substances through opening of the closed pores at high temperature in addition to the degasification of carbon during this process.

3.2. Batch method

3.2.1. Influence of pH

It is essential to realize the adsorption mechanism by determining the zero point charge (pH$_{PZC}$) of the adsorbent. The pH$_{PZC}$ of an activated carbon depends on the chemical and electronic properties of the functional groups on its surface and is a good indicator of these properties. Fig. 2 shows that the activated carbon has a pH$_{PZC}$ value of 6.3. This value means that the amount of the basic sites on the activated carbon is slightly high. Such basic character will readily adsorb protons from solution. To evaluate the effect of pH on the uptake of Fe(II) or Mn(II), batch adsorption experiments were performed at different initial pHs ranging from 1.84 to 8.3 and initial concentration 10.0 mg/L. The obtained results shown in Fig. 3(a) illustrate that the adsorption of Fe(II) or Mn(II) by activated carbon is strongly pH-dependent. Solution pH affects adsorption by regulating the adsorbent surface charge. The adsorption behavior of Fe(II) and Mn(II) over a broad pH range of 1.84–8.30 is shown in Fig. 3. It is clearly revealed that increasing solution pH showed an enhancement of adsorptive uptake of Fe(II) and Mn(II). The adsorption of cations is favored at a higher pH (>pH$_{PZC}$) while the adsorption of anions is favored at a lower pH (<pH$_{PZC}$) [26]. The maximum sorption of Fe(II) or Mn(II) is observed in the pH from 6.3 to 8.3 (pH$_{PZC}$ value of 6.3) where the surface change of WS was negative. The observed lower uptake value at low pH may be attributed to the competition of protons with the adsorption of basic active sites on the activated carbon [27]. The
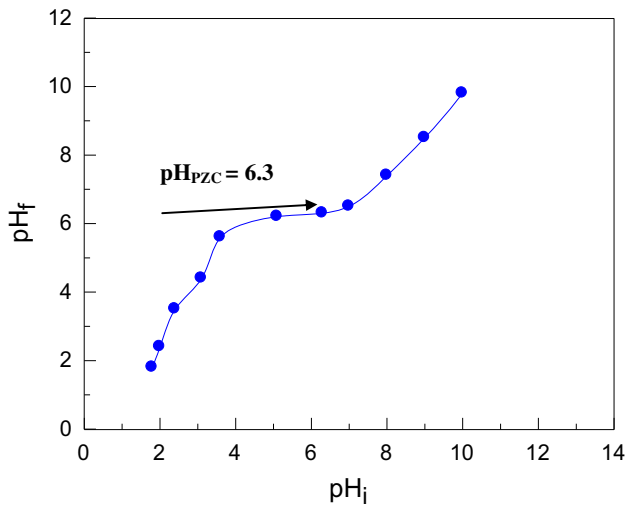
Table 1
Surface area, total pore volume, average pore diameter, iodine number, and production yield of prepared activated carbon

BET surface area (m²/g)	Total pore volume (cm³/g)	Average pore diameter (nm)	Iodine number (mg/g)	Production yield (%)
671.54	0.426	1.30	602.23	27.13

Fig. 2. Determination of pH_{PZC} of in KNO_3 solutions (pH_i, initial value; pH_f, final value).

data shown in Fig. 3(b) indicate the high efficiency of the prepared activated carbon towards the removal of Fe(II) and Mn(II), where 97.3 and 64.3% of Fe(II) and Mn(II) were removed, respectively.

3.2.2. Kinetics

To design an appropriate adsorption treatment process, it is important to understand the rate at which pollutant is removed. Therefore, the study of adsorption kinetics is crucial, as it describes the solute uptake rate which in turn controls the residence time of adsorbate uptake at the solid–solution interface. The rate of uptake of Fe(II) or Mn(II) on used carbon is rapid in the beginning and 46.85 and 43.00% of adsorption is completed in 5 min for Fe(II) and Mn(II), respectively (Fig. 4(a)). The adsorption reached the plateau after 105 min, which indicates that equilibrium has been achieved (Fig. 4 (b) and (c)). This fast rate of adsorption makes this adsorbent promising for practical applications in comparison with other reported adsorbents. The equilibrium time of some previously studied adsorbents extends from 2 h up to few days [28–30].

To better understand the adsorption kinetics of Fe(II) and Mn(II), pseudo-first-order and pseudo-second-order models were used to simulate the adsorption process. The models are expressed as follows:

(1) Pseudo-first-order model [31]:

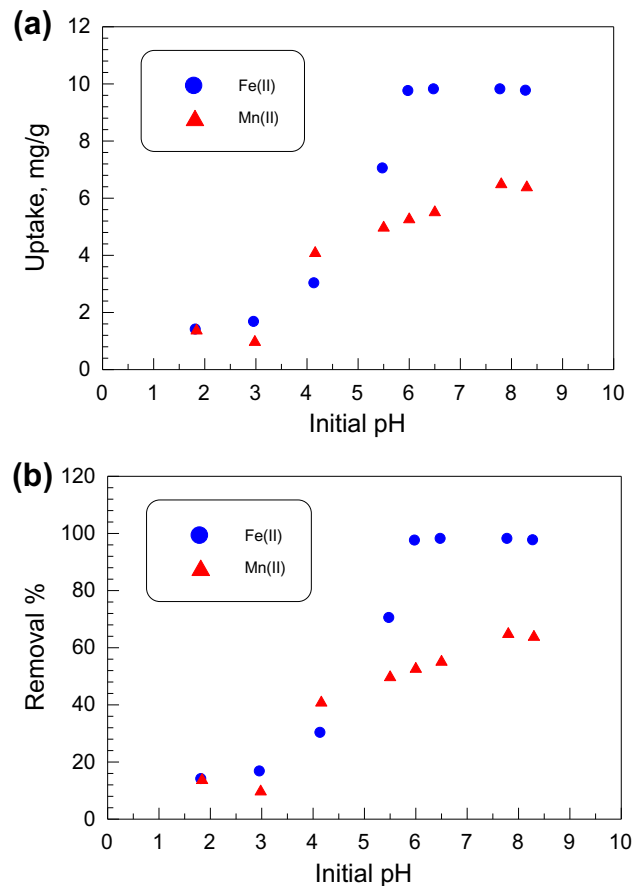$$q_t = q_e \left[1 - \exp^{-k_1 t} \right] \tag{3}$$

Fig. 3. Influence of pH on the adsorption of both Fe(II) and Mn(II) on the activated carbon at 25°C and initial concentration of 10 mg/L, (a) amount adsorbed as a function of pH, (b) removal % as a function of pH.

After linearization:

$$\log (q_e - q_t) = \log q_e - \left(\frac{k_1}{2.303} \right) t \tag{4}$$

where k_1 is the pseudo-first-order rate constant (min^{-1}) of adsorption and q_e and q_t (mg/g) are the amounts of dye adsorbed at equilibrium and time t, respectively.

(2) Pseudo-second-order model [32]:

$$q_t = \frac{k_2 t}{1 + k_2 q_e t} \tag{5}$$

After linearization:

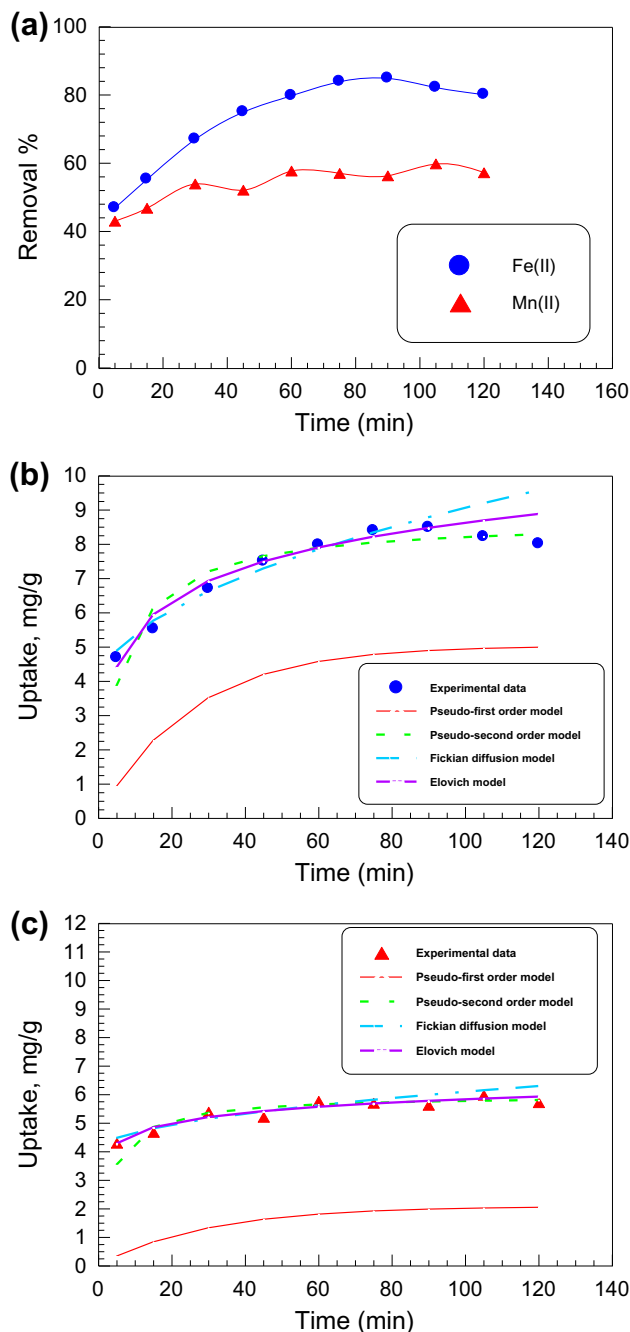$$\frac{t}{q_t} = \frac{1}{k_2 q_e^2} + \left(\frac{1}{q_e} \right) t \tag{6}$$

Fig. 4. (a) Influence of time on the removal % of both Fe(II) and Mn(II) on the activated carbon at 25°C and initial concentration of 10 mg/L, (b) amount adsorbed of Fe(II) as a function of time, (c) amount adsorbed of Mn(II) as a function of time.

where k_2 is the pseudo-second-order rate constant of adsorption (g/mg min). The kinetic parameters in both two models are determined from the linear plots of log $(q_e - q_t)$ vs. t for pseudo-first-order (Fig. 5(a)) or (t/q_t) vs. t for pseudo-second-order (Fig. 5(b)). The
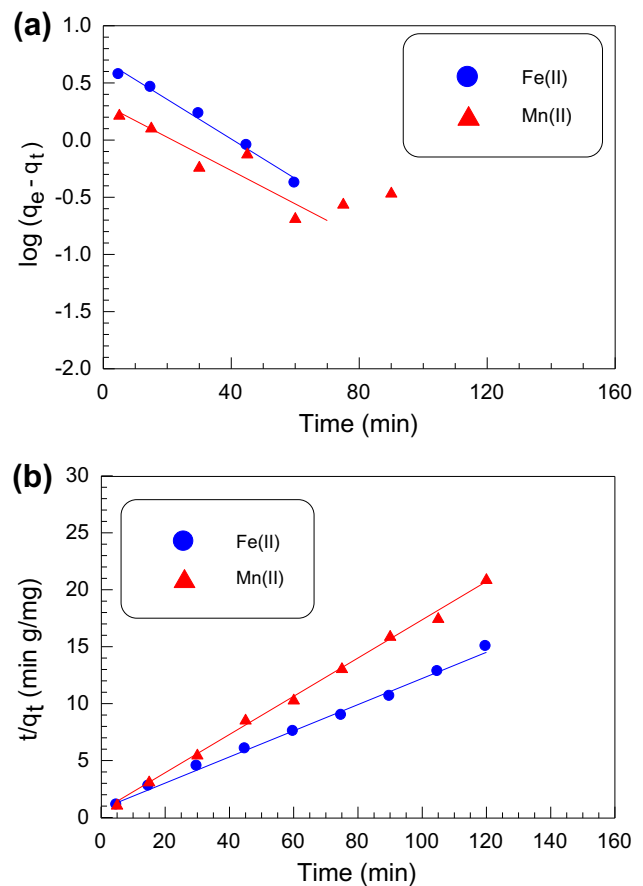

Fig. 5. (a) Linear pseudo-first-order and (b) linear pseudo-second-order kinetic models for the adsorption of both Fe(II) and Mn(II) on the activated carbon.

validity of each model is checked by the fitness of the straight line (R^2) as well as the experimental and calculated values of q_e. Accordingly, and as shown in Table 2, it can be found that the adsorption kinetics data are well described by pseudo-second-order rate model (R^2 above 0.99).

The adsorption kinetics study is helpful to understand the mechanism of adsorption reactions. The pseudo-second-order kinetic model is based on the assumption that the rate-limiting step may be chemisorption involving valency forces through sharing or exchange of electrons between sorbent and sorbate [33,34], which is suitable for sorption at low initial concentration. It was found that the kinetic experimental data obtained could be best fitted into the pseudo-second-order rate model. This observation suggests that Fe(II) or Mn(II) adsorption onto carbon particles involves chemisorption.

Most adsorption reactions take place through multistep mechanism comprising (1) external film diffusion, (2) intraparticle diffusion, and (3) interaction

Table 2
Kinetic parameters of the adsorption of Fe(II) and Mn(II) on the activated carbon

Metal ion	Pseudo-first-order			Pseudo-second-order			Fickian diffusion law			Elovich equation		
	k_1 (min^{-1})	$q_{e,\,calc}$ (mg/g)	R^2	k_2 (g/mg min)	$q_{e,\,calc}$ (mg/g)	R^2	K_i (mg/g min$^{-0.5}$)	X	R^2	α (mg/g min)	β (g/mg)	R^2
Fe(II)	0.039	5.021	0.988	0.018	8.713	0.995	0.538	3.665	0.966	6.290	0.708	0.973
Mn(II)	0.033	2.066	0.843	0.048	5.962	0.997	0.208	3.993	0.806	389.478	1.930	0.910

between adsorbate and active site. Since the first step is excluded by shaking the solution, the rate determining step is one of the other two steps. To know if the intraparticle diffusion is the rate-determining step or not the uptake/time data were treated according to Fickian diffusion law [35].

$$q_t = K_i t^{0.5} + X \qquad (7)$$

where q_t is the amount of dye adsorbed at time t and K_i is the intraparticle diffusion rate (mg/g min$^{-0.5}$). The K_i is the slope of straight-line portions of the plot of q_t vs. $t^{0.5}$. The plot of qt against $t^{0.5}$ gave two straight-line portions with two different slopes and intercept values (Fig. 6(a)). The K_i values obtained from the slope of the first straight-line portion are 0.538 and 0.208 (mmol/g min$^{-0.5}$), for Fe(II) and Mn(II), respectively. This high value of K_i indicates the fast transfer. The positive values of X 3.665 and 3.993 for Fe(II) and Mn(II), respectively, indicate boundary layer effect on the rate of adsorption. The higher value of X for Mn(II) than Fe(II) indicates the higher boundary layer effect in case of Mn(II) adsorption, which explains the lower uptake of Mn(II) than Fe(II).

Elovich equation was also applied to the sorption of Fe(II) and Mn(II) by the activated carbon according to the relation [36]:

$$q_t = 1/\beta \ln(\alpha\beta) + 1/\beta \ln t \qquad (8)$$

where q_t is the sorption capacity at time t, α the initial sorption rate (mmol/g min), and β the desorption constant (g/mg). Thus, the constants can be obtained from the slope and intercept of a straight line plot of q_t vs. log t (Fig. 6(b)). The linearization of the equation giving the rate of reaction allows obtaining the initial sorption rate, α (mg/g min) from the intercept of a straight line plot of q_t vs. ln t (Fig. 6(b)). The values of α for the adsorption of Fe(II) and Mn(II) on the carbon are 6.290 and 389.478 (mg/g min), respectively. These values indicate that the initial adsorption rate of Mn(II) is higher than that of Fe(II). The
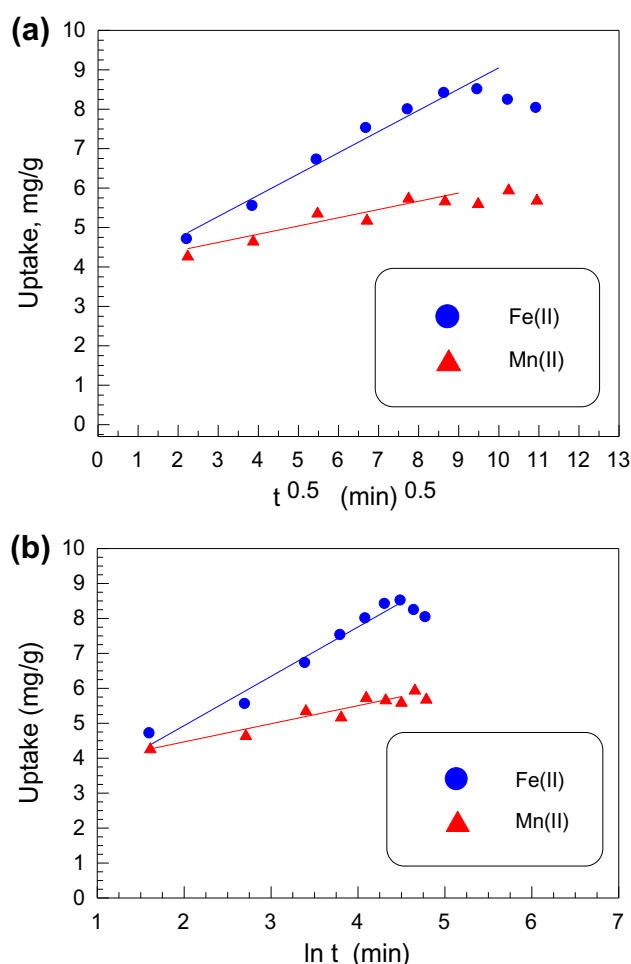

Fig. 6. (a) Linear Fickian diffusion and (b) linear Elovich kinetic models for the adsorption of both Fe(II) and Mn(II) on the studied carbon.

values of β (desorption constant) are found to be 0.708 and 1.930 g/mg, for Fe(II) and Mn(II), respectively. These values explain the higher affinity of the carbon towards Fe(II) than Mn(II). The data obtained indicate that the studied carbon is promising for Fe(II) and Mn(II) removal.

3.2.3. Influence of adsorbent dose

The amount of carbon used for adsorption experiments was varied from 0.01 to 0.15 g in 50 mL volume at an initial concentration of 10 ppm; contact time of 1 h at 25 ± 1℃, and pH 6.5 for both Fe(II) and Mn(II). The results, as shown in Fig. 7, reveal that percent removal and uptake (mg/g) values show opposite trends. The observed increase in percent removal with sorbent dose increase can be simply attributed to the fact that increase in amount of sorbent result in increase in surface area thus providing more and more binding sites for both Fe(II) and Mn(II) uptake. This finally results in enhancement in percent uptake. However, the decrease in the value of the uptake (mg/g) with sorbent dose may be explained as follows: it is clear from Fig. 7(b) that with increase in sorbent dose from 0.01 to 0.15 g, the percent uptake increases from 50.11 to 91.72 for Fe(II), and from 30.8 to 70.4 for Mn(II). This data suggest that difference between final and initial concentration do not increase
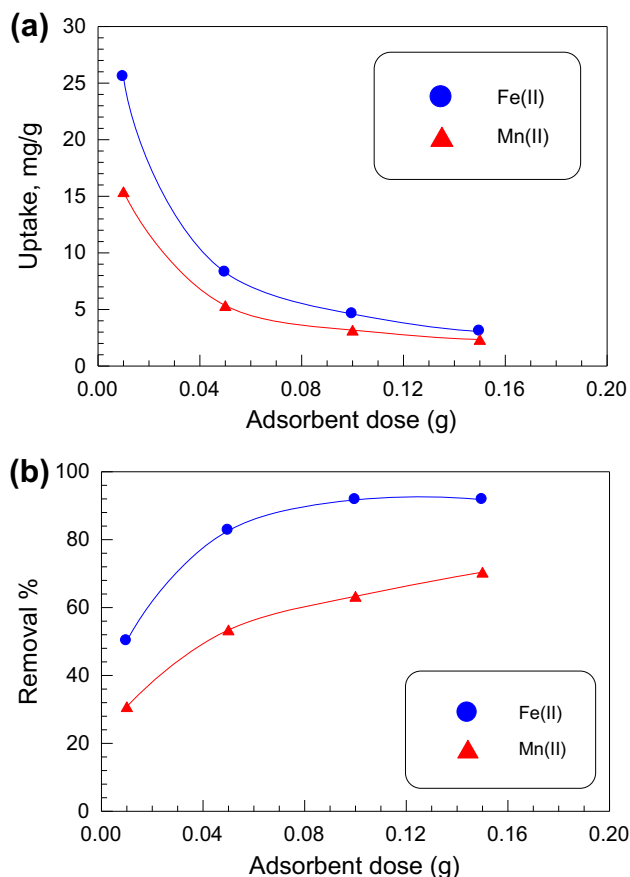
in the same proportion as that of adsorbent dose increases. The overall effect of this marginal increase in "x" value is that uptake decreased gradually. Thus the optimum adsorbent amount of activated carbon was found as 0.1 g by the given uptake (mg/g) and removal percent.

3.2.4. Equilibrium adsorption isotherm

Study on Fe(II) and Mn(II) adsorption isotherm was conducted at pH 6.5 ± 0.1, the optimal pH for both Fe(II) and Mn(II) adsorption on the prepared carbon (Fig. 8). Obviously, increasing the concentration Fe(II) or Mn(II) involves an increase in the uptake of Fe(II) and Mn(II). Both Langmuir and Freundlich isotherm models were used to describe the relationship between the amount of Fe(II) or Mn(II) adsorbed and its equilibrium concentration in aqueous solution. Langmuir model is applicable to homogeneous sorption, which the adsorption of each adsorbate molecule onto the sorbent has equal adsorption activation energy. Langmuir model can be expressed by the following equation [37]:

$$q_e = \frac{Q_{max} K_L C_e}{1 + K_L C_e} \tag{9}$$

where q_e the adsorbed value of dyes at equilibrium concentration (mg/g), Q_{max} is the maximum adsorption capacity (mg/g), and K_L is the Langmuir binding constant which is related to the energy of adsorption (L/mg), C_e is the equilibrium concentration of metal ion in solution (mmol/L).
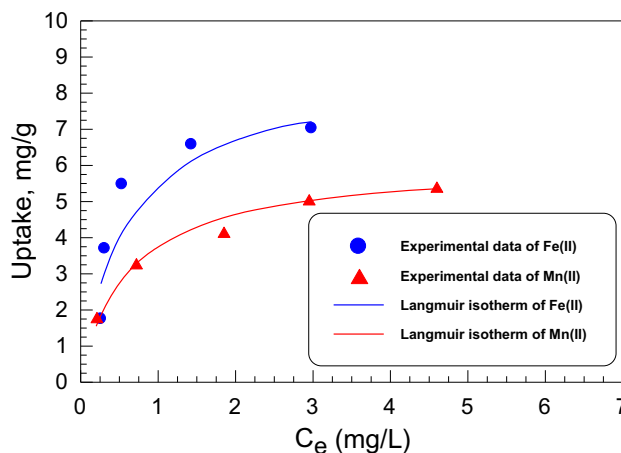

Fig. 7. Influence of adsorbent dose on the adsorption of both Fe(II) and Mn(II) on the activated carbon at 25℃ and initial concentration of 10 mg/L, (a) amount adsorbed as a function of pH, (b) removal % as a function of pH.

Fig. 8. Non linear Langmuir isotherms for the adsorption of both Fe(II) and Mn(II) on the activated carbon at pH 6.5 and 25℃.

After linearization:

$$\frac{C_e}{q_e} = \frac{C_e}{Q_{max}} + \frac{1}{K_L Q_{max}} \qquad (10)$$

The most important multisided adsorption isotherm for heterogeneous surfaces is the Freundlich isotherm, characterized by the heterogeneity factor $1/n$. The Freundlich model is described by [38]:

$$q_e = K_F C_e^{1/n} \qquad (11)$$

where K_F and n are the Freundlich constants related to the adsorption capacity and intensity, respectively. After linearization:

$$\log q_e = \log K_F - \frac{1}{n} \log C_e \qquad (12)$$

The values of K_L, Q_{max}, K_F, and n at different temperatures are calculated from Fig. 9 and reported in Table 3. The maximum adsorption capacities (Q_{max}) obtained at different temperatures are in good agreement with the experimental ones, and the values of R^2 reported in Table 3, which is a measure of the goodness-of-fit, confirm the better representation of the experimental data by Langmuir model than Freundlich model. This indicates the homogeneity of active sites on the adsorbent surface.

The degree of suitability of the obtained adsorbents towards dyes was estimated from the values of the separation factor (R_L) using the following relation [39]:

$$R_L = \frac{1}{1 + K_L C_0} \qquad (13)$$

where K_L is the Langmuir equilibrium constant and C_0 is the initial concentration of dye. Values of $0 < R_L < 1$ indicates the suitability of the process. The values of R_L for the investigated adsorbent towards the adsorption of both Fe(II) and Mn(II) lie between 0.09 and 0.20 for all concentration and temperature ranges. This implies that the adsorption of both Fe(II) and Mn(II) on the prepared activated carbon from aqueous solution is favorable under the conditions used in this study.

3.2.5. Influence of temperature

Adsorption capacities were established for both Fe(II) and Mn(II) at temperatures varying between 20 and 50°C (Fig. 10). A slight increase in sorption capacity can be observed, especially at 40–50°C. The maximum sorption capacity increased between 20 and 50°C
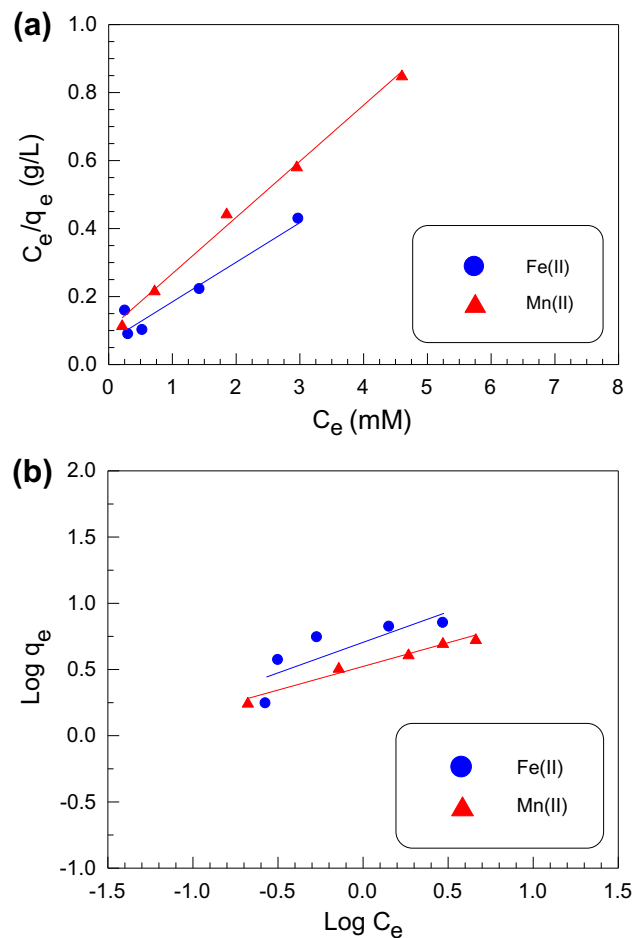
Fig. 9. (a) Linear Langmuir and (b) linear Freundlich isotherms for the adsorption of both Fe(II) and Mn(II) on the activated carbon at pH 6.5 and 25°C.

by 29.8 and 12.9% for Fe(II) and Mn(II), respectively with increasing the temperature to 50°C. This means that the adsorption is endothermic in nature [10]. The thermodynamic parameters including Gibbs free energy ($\Delta G°$), enthalpy ($\Delta H°$), and entropy ($\Delta S°$) for the adsorption of Fe(II) and Mn(II) onto activated carbon have been calculated by using equations as follows and presented in Table 4 [10,13]:

$$K_C = \frac{C_A}{C_S} \qquad (14)$$

$$\ln K_C = \frac{-\Delta H°}{RT} + \frac{\Delta S°}{R} \qquad (15)$$

$$\Delta G° = \Delta H° - T\Delta S° \qquad (16)$$

where K_C is the equilibrium constant, C_S is the equilibrium concentration of the metal ion in the solution

Table 3
Langmuir and Freundlich constants for adsorption the adsorption of Fe(II) and Mn(II) on the activated carbon

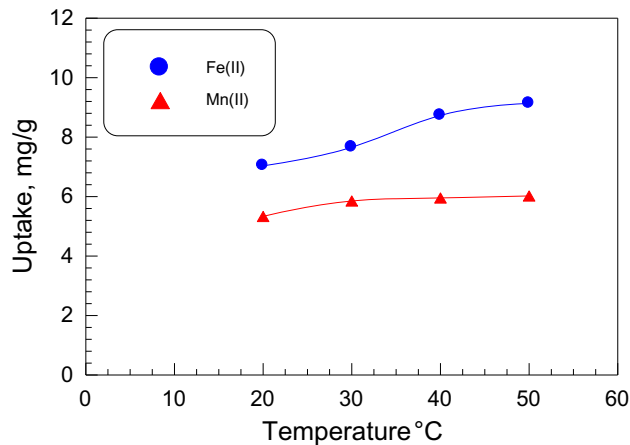| Metal ion	Langmuir constants				Freundlich constants		
	$Q_{\text{max,exp}}$ (mg/g)	$Q_{\text{max,calc}}$ (mg/g)	K_L (L/mg)	R^2	n	K_F	R^2
Fe(II)	7.01	8.600	1.701	0.935	2.169	5.067	0.674
Mn(II)	5.40	6.054	1.611	0.994	2.797	3.334	0.975

Fig. 10. Influence of temperature on the adsorption of both Fe(II) and Mn(II) on the activated carbon at pH 6.5 and 25°C.
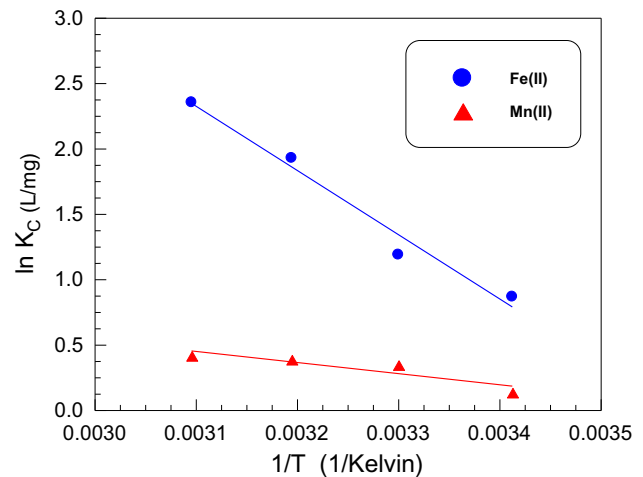

Fig. 11. Van't Hoff plots for adsorption of Fe(II) and Mn (II) on the activated carbon.

(mg/L), C_A the amount of metal ion adsorbed on the adsorbent in the solution at equilibrium (mg/L). R is the gas constant and T is the solution temperature (K). $\Delta S°$ and $\Delta H°$ were obtained from the intercept and slope of Van't Hoff plot of ln K_C vs. $1/T$ (Fig. 11) from Eq. (15). The results are given in Table 4. The negative values of $\Delta G°$ indicated the feasibility and spontaneous nature of Fe(II) and Mn(II) sorption onto activated carbon. The value of enthalpy of a sorption process is used to determine the chemical or physical sorption. For chemical sorption enthalpy values vary from 83 to 830 kJ/mol, and for physical sorption they vary from 8 to 25 kJ/mol [26]. It can be concluded from the low

values of $\Delta H°$ that the interaction between Fe(II) and Mn(II) and activated carbon is physical. The endothermic nature is also indicated by the positive value of $\Delta H°$. Generally, $\Delta G°$ values range from 0 to −20 KJ/mol for physical adsorption and −80 to −400 KJ/mol for chemical adsorptions [26]. In this study, the $\Delta G°$ values ranged from −0.44 to −6.29 KJ/mol, indicating that adsorption is mainly physical.

3.2.6. Influence of ionic strength and agitation speed

Influence of ionic strength and agitation speed on adsorption of both Fe(II) and Mn(II) were carried out

Table 4
Enthalpy, entropy, and free energy changes for adsorption of Fe(II) and Mn(II) on the activated carbon

Metal ion	$\Delta H°$ (kJ/mol)	$\Delta S°$ (kJ/mol K)	$\Delta G°$ (kJ/mol)			
			293 K	303 K	313 K	323 K
Fe(II)	40.836	0.145	−1.916	−3.375	−4.834	−6.293
Mn(II)	7.062	0.025	−0.440	−0.696	−0.953	−1.209

with shaker at pH 6.5, initial concentration solution was 10 ppm, contact time 60 min, and adsorbent dose was 0.05 g in 50 mL volume.

Ionic strength is one of the important factors influencing aqueous phase equilibrium. The effects of the interfering chloride anions were evaluated for both Fe(II) and Mn(II) adsorption. Adsorption of Fe(II) did not influenced by increasing amount of NaCl from 0.2 to 1 g (Fig. 12(a)), However, the adsorption of Mn(II) was slightly decreased by increasing ionic strength of the dissolved phase.

The agitation speed varied from 0.5 to 4 rpm. The adsorption rate increased because of increasing kinetic energy of both Fe(II) and Mn(II) particles (Fig. 12(b)). Thus, the adsorption efficiency increased with increase in agitation speed and adsorption efficiency was maximal at 2 rpm for both Fe(II) and Mn(II). It was observed that adsorption efficiency decreased at 4 rpm, this may be due to the increase of desorption rate at high agitation speed.

3.3. Column studies

3.3.1. Loading of the column

Breakthrough curves of the studied carbon towards adsorption of both Fe(II) and Mn(II) at flow rate of 2 mL/min and a fixed bed height (2.65 cm) indicate that, the breakthrough time of Fe(II) is higher than that of Mn(II) (Fig. 13). This behavior of breakthrough time values is consistent with the reported adsorption capacity obtained from batch method. The column adsorption capacities are 7.71 and 5.95 mg/g for Fe(II) and Mn(II), respectively. It is worth to mention that the column adsorption capacities are slightly higher than that obtained from the corresponding batch method (7.01 and 5.40 mg/g for Fe(II) and Mn(II)). This may be attributed to the lower desorption rate in the last case.
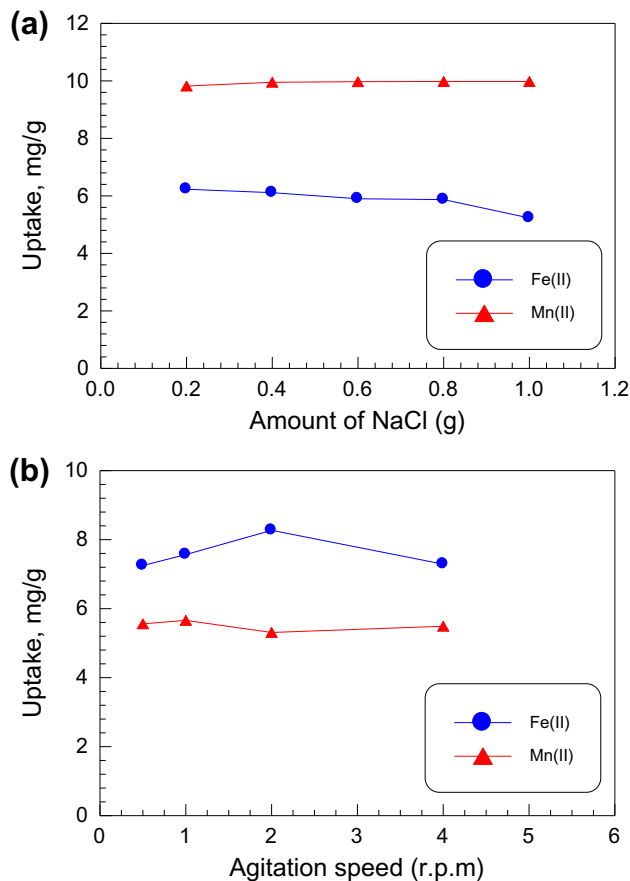

Fig. 12. (a) Influence of ionic strength and (b) influence of agitation speed on the adsorption of both Fe(II) and Mn(II) on the activated carbon at pH 6.5 and 25°C.
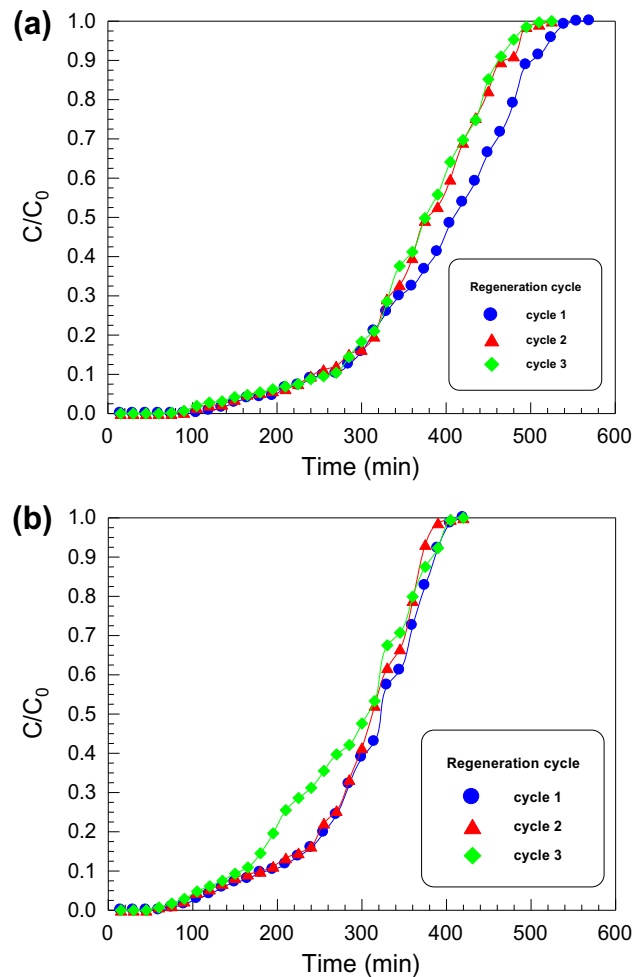

Fig. 13. (a) Influence of successive desorption cycles on the breakthrough curves for the removal of Fe(II) and (b) for Mn(II) at flow rate of 2 mL/min and bed height of 2.65 cm.

3.3.2. Regeneration of the column

Sorption/desorption cycle runs were carried out for both Fe(II) and Mn(II) on the obtained carbon. The elution of Fe(II) and Mn(II) ions was performed using 50 mL 0.5 M of hydrochloric acid. As shown in Fig. 13, the breakthrough curves for recovery of Fe(II) and Mn(II) (flow rate of 2 mL/min, bed height 2.65 cm) showed no characteristic changes during successive cycles. This indicates that activated carbon has good performance for repeated use up to three cycles. The RE of Fe(II) was found to be 93.64 and 92.67% for three successive sorption cycles, respectively. Whereas, the RE of Mn(II) was found to be 96.81 and 91.68% for three successive sorption cycles, respectively.

4. Conclusion

Activated carbon was prepared from sugarcane bagasse impregnated with phosphoric acid at 500°C. The adsorbent obtained is characterized by its high BET surface area and pore volume. The activated carbon showed fast and high removal efficiency for Fe(II) and Mn(II) from aqueous medium at approximately pH 6.5 ± 0.1. The removal efficiency of Fe(II) and Mn(II) ions was found to be highly dependent upon the acidity of the medium. The adsorption was found to be pseudo-second-order kinetics, proceeds according to Langmuir isotherm, endothermic in nature and mainly physical. The uptake values of 7.01 and 5.40 mg/g for Fe(II) and Mn(II) were reported at 25°C, respectively. Column studies give an account about the breakthrough points at flow rate 2 mL/min and bed height 2.65 cm. Column adsorption capacity is slightly higher than that obtained from the corresponding batch method. The RE of Fe(II) was found to be 93.64 and 92.67% for three successive sorption cycles, respectively. Whereas the RE of Mn(II) was found to be 96.81 and 91.68% for three successive sorption cycles, respectively.

References

[1] J.O. Ogunbileje, V.-M. Sadagoparamanujam, J.I. Anetor, E.O. Farombi, O.M. Akinosun, A.O. Okorodudu, Lead, mercury, cadmium, chromium, nickel, copper, zinc, calcium, iron, manganese and chromium (VI) levels in Nigeria and United States of America cement dust, Chemosphere 90 (2013) 2743–2749.

[2] E.A. Smith, P. Newland, K.G. Bestwick, N. Ahmed, Increased whole blood manganese concentrations observed in children with iron deficiency anaemia, J. Trace Elem. Med. Biol. 27 (2013) 65–69.

[3] K. Vaaramaa, J. Lehto, Removal of metals and anions from drinking water by ion exchange, Desalination 155 (2003) 157–170.

[4] A. Ali, H. Shawky, H. Abd El Rehim, E. Hegazy, Synthesis and characterization of PVP/AAc copolymer hydrogel and its applications in the removal of heavy metals from aqueous solution, Eur. Polym. J. 39 (2003) 2337–2344.

[5] World Health Organization, Guidelines for Drinking Water Quality, vol. 1, Recommendations, Geneva, 1984 p. 79.

[6] M.G. Salem, M.H. El-Awady, E. Amin, Enhanced removal of dissolved iron and manganese from non-conventional water resources in delta district, Egypt Energy Procedia 18 (2012) 983–993.

[7] M.M. Khin, A.S. Nair, V.J. Babu, R. Murugan, S. Ramakrishna, A review on nanomaterials for environmental remediation, Energy Environ. Sci. 5 (2012) 8075–8109.

[8] C. Zhang, Q. Wang, H. Li, J. Lu, Remediation of iron, manganese, and organic pollutants in lignite-derived water using an upflow biological aerated filter, Clean-Soil Air Water 41 (2013) 365–369.

[9] C. Gerente, V.K.C. Lee, P. Cloirec, G. McKay, Application of chitosan for the removal of metals from wastewaters by adsorption-mechanisms and models review, Crit. Rev. Environ. Sci. Technol. 37 (2007) 41–127.

[10] M.M.H. Khalil, K.Z. Al-Wakeel, S.S. Abd El-Rehim, H. Abd El-Monem, Efficient removal of ferric ions from aqueous medium by amine modified chitosan resins, J. Environ. Chem. Eng. 1 (2013) 566–573.

[11] A. Bhatnagar, E. Kumar, M. Sillanpää, Fluoride removal from water by adsorption – A review, Chem. Eng. J. 171 (2011) 811–840.

[12] M. Gallegos-Garcia, K. Ramírez-Muñiz, S. Song, Arsenic removal from water by adsorption using iron oxide minerals as adsorbents: A review, Miner. Process. Extr. Metall. Rev. 33 (2012) 301–315.

[13] M.M.H. Khalil, K.Z. Al-Wakeel, S.S. Abd El Rehim, H. Abd El Monem, Adsorption of Fe(III) from aqueous medium onto glycine-modified chitosan resin: Equilibrium and kinetic studies, J. Dispersion Sci. Technol., http://www.tandfonline.com/doi/abs/10.1080/01932691.2013.859624#.U21ktvmSyTQ

[14] S. Li, S. Xie, C. Zhao, Y. Zhang, J. Liu, T. Cai, Efficiency of adsorption of wastewater containing uranium by fly ash, Adv. Mater. Res. 639–640(1) (2013) 1295–1299.

[15] Y.-S. Ho, Effect of pH on lead removal from water using tree fern as the sorbent, Bioresour. Technol. 96 (2005) 1292–1296.

[16] J. Kyzioł-Komosińska, I. Twardowska, A. Kocela, Adsorption of cadmium(II) ions from industrial wastewater by low moor peat occurring in the overburden of brown coal deposits, Arch. Environ. Protect. 34 (2008) 83–94.

[17] K.Z. Elwakeel, M.A. Abd El-Ghaffar, S.M. El-Kousy, H.G. El-Shorbagy, Synthesis of new ammonium chitosan derivatives and their application for dye removal from aqueous media, Chem. Eng. J. 203 (2012) 458–468.

[18] H. Guedidi, L. Reinert, J.-M. Lévêque, Y. Soneda, N. Bellakhal, L. Duclaux, The effects of the surface oxidation of activated carbon, the solution pH and the temperature on adsorption of ibuprofen, Carbon 54 (2013) 432–443.

[19] O.G. Apul, Q. Wang, Y. Zhou, T. Karanfil, Adsorption of aromatic organic contaminants by graphene nanosheets: Comparison with carbon nanotubes and activated carbon, Water Res. 47 (2013) 1648–1654.

[20] F.-F. Liu, J.-L. Fan, S.-G. Wang, G.-H. Ma, Adsorption of natural organic matter analogues by multi-walled carbon nanotubes: Comparison with powdered activated carbon, Chem. Eng. J. 219 (2013) 450–458.

[21] T. Adinaveen, L.J. Kennedy, J.J. Vijaya, G. Sekaran, Studies on structural, morphological, electrical and electrochemical properties of activated carbon prepared from sugarcane bagasse, J. Ind. Eng. Chem. 19 (2013) 1470–1476.

[22] K.Y. Foo, L.K. Lee, B.H. Hameed, Preparation of activated carbon from sugarcane bagasse by microwave assisted activation for the remediation of semi-aerobic landfill leachate, Bioresour. Technol. 134 (2013) 166–172.

[23] B.S. Girgis, I.Y. El-Sherif, A.A. Attia, N.A. Fathy, Textural and adsorption characteristics of carbon xerogel adsorbents for removal of Cu(II) ions from aqueous solution, J. Non-Cryst. Solids 358 (2012) 741–747.

[24] J.S. Noh, J.A. Schwarz, Estimation of surface ionization constants for amphoteric solids, J. Colloid Interface Sci. 139 (1990) 139–148.

[25] APHA, Standard Methods for the Examination of Water and Wastewater, 20th ed., American Public Health Association, Washington, DC, 1918.

[26] V. Govindasmay, R. Sahadevan, S. Subramanian, D.K. Mahendradas, Removal of malachite green from aqueous solution by perlite, Int. J. Chem. Reactor. Eng 7 (2009) 43–49.

[27] A.A. Atia, A.M. Donia, K.Z. Elwakeel, Adsorption behaviour of non-transition metal ions on a synthetic chelating resin bearing iminoacetate functions, Sep. Purif. Technol. 43 (2005) 43–48.

[28] P. Mondal, C.B. Majumder, B. Mohanty, Treatment of arsenic contaminated water in a batch reactor by using *Ralstonia eutropha* MTCC 2487 and granular activated carbon, J. Hazard. Mater. 153 (2008) 588–599.

[29] M.A. Abd El-Ghaffar, Z.H. Abdel-Wahab, K.Z. Elwakeel, Extraction and separation studies of silver(I) and copper (II) from their aqueous solution using chemically modified melamine resins, Hydrometallurgy 96 (2009) 27–34.

[30] L. Huang, J. Kong, W. Wang, C. Zhang, S. Niu, B. Gao, Study on Fe(III) and Mn(II) modified activated carbons derived from *Zizania latifolia* to removal basic fuchsin, Desalination 286 (2012) 268–276.

[31] S. Lagergren, About the theory of so-called adsorption of soluble substances, Kungliga Svenska Vetenskapsakademiens, Handlingar 24 (1898) 1–39.

[32] Y.S. Ho, G. McKay, Pseudo-second order model for sorption processes, Process Biochem. 34 (1999) 451–465.

[33] S. Azizian, Kinetic models of sorption: A theoretical analysis, J. Colloid Interface Sci. 276 (2004) 47–52.

[34] H. Cui, Q. Li, S. Gao, J.K. Shang, Strong adsorption of arsenic species by amorphous zirconium oxide nanoparticles, J. Ind. Eng. Chem. 18 (2012) 1418–1427.

[35] K.Z. Elwakeel, Removal of Cr(VI) from alkaline aqueous solutions using chemically modified magnetic chitosan resins, Desalination 250 (2010) 105–112.

[36] K.Z. Elwakeel, M. Rekaby, Efficient removal of Reactive Black 5 from aqueous media using glycidyl methacrylate resin modified with tetraethelenepentamine, J. Hazard. Mater. 188 (2011) 10–18.

[37] I. Langmuir, The adsorption of gases on plane surfaces of glass, mica and platinum, J. Am. Chem. Soc. 40 (1918) 1361–1403.

[38] H.M.F. Freundlich, Uber die adsorption in losungen [Over the adsorption in solution], Z. J. Phys. Chem. 57 (1906) 385–470.

[39] L. Qi, Z. Xu, Lead sorption from aqueous solutions on chitosan nanoparticles, Colloids Surf. A 251 (2004) 186–193.